

Study of Vacuum Residues and Their Transformation to Asphalts for the Pavement Industry by Nuclear Magnetic Resonance and **Chemometric Methods**

Leonardo Jaimes M., † Nicolas Santos S., ‡ and Daniel Molina V.*, † [8]

[†]Laboratorio de Resonancia Magnética Nuclear, and [‡]Grupo de Investigación en Tomografía Computarizada para Caracterización de Yacimientos - GIT, Universidad Industrial de Santander, Apartado Aereo 678, Bucaramanga, 680002 Colombia

ABSTRACT: This paper reports the findings of a one-year long study, that every week measured the physicochemical properties (P: penetration; A: softening; Ip: penetration index; V: rotational viscosity, R: mass loss), and the spectroscopic and the relaxometry properties via nuclear magnetic resonance, of the vacuum residues (VR) produced in a refinery and those modified into asphalts to fabricate pavements with penetration grade 60/70. The evolution of the structural changes, along the time of study, was measured via high-field and low-field ¹H NMR and analyzed through multivariate statistical methods. The attained results with high-field ¹H NMR showed that when the VR are oxidized, the proportion of protons associated with the high-molecular-weight polyaromatic increases. On the other hand, the low-field ¹H NMR results, through a greater number of unimodal distribution plots of T2 relaxation time, showed the homogenization of the aggregation as well as of the dynamic properties of the molecules, thus indicating that the aging of asphalts cannot be prevented despite the treatment. After analysis of the physicochemical properties, it was found that some refinery VR samples do not meet the quality specifications of penetration grade 60/70, dictated by the National Roads Institute of Colombia (INVIAS), to be employed as raw material in the manufacturing of pavements, but only after being processed and modified.

1. INTRODUCTION

Crude oils that arrive into the refineries are not generally segregated crudes but blends with changing properties and composition over time. The same behavior is followed by the characteristics of the fractions and products obtained after refinement. Therefore, their properties have to be permanently measured and tracked, in order to meet the quality specifications. Some of these refinement fractions are the socalled vacuum residues (VR), which are conventionally used as raw material for the production of pavements. The VR are the fractions of crude oils that do not distill at atmospheric pressure nor at vacuum pressure, 1,2 and their chemical composition is very complex, with a solid n-heptane insoluble portion, so-called asphaltenes (9-29% w/w), and another liquid portion, known as maltenes. The VR properties depend on their chemical composition, their structural characteristics at the molecular level, on how they are obtained, and specifically on the crude oil they come from.

The VR are also generally called asphalt. This term is employed in a similar way to refer to bitumen, particularly in Europe. According to the ASTM D8-18 standard, for road and pavement materials, asphalt is obtained by means of atmospheric distillation, vacuum distillation, and steamdistillation processes. Sometimes, additional distillation processes may be necessary to obtain a residual whose physical properties are appropriate for commercial applications. These additional processes include air oxidation, dissolvent elimination, or blending of residues with different characteristics.

The characterization of the physical and chemical properties of crude oils and their fractions is of great importance for the oil industry to determine their potential application. The theory of continuous change in the composition of petroleum was demonstrated in the 1990s. It showed a gradual and continuous increase with respect to aromaticity, molecular weight, and the content of heteroatoms (Boduszynski's continuous model)³ and also a continuous change when interpolating or extrapolating the physical and chemical properties of the oil fractions. Further, different strategies for the selection and interpretation of the analytical measurements, taken over ultraheavy oils fractions, were proposed.⁴

In recent years, exhaustive characterization by means of Fourier-transform ion cyclotron resonance mass spectrometry (FT-ICR MS) provided composition data which strongly supported the continuous method. However, the molecular formulas obtained via FT-ICR MS for the distillates and asphaltenes of the same crude oil showed a gap between the compositional space of "asphaltenes" and "maltenes", thus contradicting the model of Boduszynski-Altgelt. Previous tests indicated that the observed discontinuities for the polar fractions, such as asphaltenes and resins, are caused by the aggregation of their components and that nanoaggregates of asphaltenes represent the insoluble components.

As an alternative, different analytical and molecular spectroscopy techniques have been proposed including gas chromatography (GC), high-performance liquid chromatography (HPLC), thin-layer chromatography (TLC), infrared spectroscopy (IR), Raman spectroscopy, nuclear magnetic resonance (NMR) spectroscopy, and mass spectroscopy (MS). According to Akrami, Yardim, and Ekinci, through Raman spectroscopy, the chemical features of heavy oils have

Received: December 1, 2018 Revised: January 19, 2019 Published: January 22, 2019



been classified as an extreme aromatic intermediate based on their high content of asphaltenes and sulfur.

Nowadays, nuclear magnetic resonance spectroscopy is one of the most powerful tools for the analysis of complex organic molecular blends and for the prediction of their properties. Further, it is nondestructive and requires short test times. Proton NMR (¹H NMR) is the most widely used due to its high sensitivity, which comes from the fact that the proton has the largest nuclear magnetic momentum, and almost 100% isotopic abundance. NMR has been used in the compositional analysis of heavy oil fractions for a long time, since the first published work by Friedel in 1959.⁹

High-resolution ¹H and ¹³C NMR have been used in the analysis of VR in the past, including different studies about the structural parameters of asphalts, ¹⁰ structural changes during asphalt oxidation, ¹¹ chemical transformations during Arab asphalts aging, ¹² studies of the amorphous and crystalline phases of asphalts, ¹³ the percentage of aromatics and aromatic substitution of asphalts, ¹⁴ the chemical and rheological properties of modified asphalts, ¹⁵ and the characteristics and distribution of the functional groups before and after aging of modified asphalt with crumb rubber (CR) and the addition of styrene—butadiene—styrene (SBS) and sulfur. ¹⁶

Low-resolution 1 H NMR has been used to measure the relaxometric properties of crude oils, throughout their T_1 and T_2 relaxation times and their diffusion, which are employed to study some properties and features including porous structures in asphaltic cements, 17 changes in the activation energies of asphalts with different sulfur concentrations, 18 viscosity and asphalts aging, 19 relative viscosity of binder in asphalt concrete without the need for binder extraction, 20 the effect of recycled materials and recycling agents in asphalt blends samples, 21 the effect of modifiers on the bitumen microstructure aging process, 22 the monitoring of the long-term aging of asphalt binder in mixture cores without binder extraction, 23 and the softening point and their response to specific conditions of bitumen which has been doped by different percentages of polyphosphoric acid (PPA).

In this paper, a study of the physicochemical, spectroscopic, and relaxometric properties of the VR produced in refinery and those modified into asphalts to fabricate pavements, which were measured weekly, for one year long is reported. The $^1\mathrm{H}$ NMR spectra and the T_2 relaxation times were employed to assess the changes in the composition and molecular aggregation, respectively. The significant variables among the physicochemical properties of VR were selected by means of the Pearson and Spearman correlation coefficients, and the data variability was determined via principal components analysis (PCA).

2. EXPERIMENTAL SECTION

2.1. Preparation of the Samples and Physicochemical Characterization. The vacuum residues employed in this paper were produced by the ECOPETROL S.A. refinery, located in Barrancabermeja, Colombia, and they were transformed into asphalts by the company Manufactura y Procesos Industriales (MPI). Sixtyfour samples were collected, one per week, during one year. The VR were processed in the MPI's facility through heating in the presence of oxygen plus additives (details of the treatment are omitted due to industrial secret issues), and their properties were modified in order to meet the specifications of the pavements industry (penetration grade 60/70). The original VR from ECOPETROL are identified with the abbreviation ECP (1–64 samples) and the ones processed in MPI are

identified as MPI (1–64 samples) for a total of 128 samples. They are also referred to as nonaged and aged VR, respectively.

The following physicochemical properties were determined for all the samples: penetration (P), softening (A), penetration index (Ip), rotational viscosity (V), and mass loss (R). Additionally, penetration (PR), softening (AR), and rotational viscosity (VR) were determined for residues obtained via RTFOT, which is a process that ages the samples in an oven at 163 °C, using cylindrical glass containers that rotate and create a fine asphalt film exposed continuously to air, in order to accelerate the loss of volatiles and the oxidation during 85 min. This procedure simulates the oxidation that occurs during the mixing and placing of the asphaltic pavement on roads.

The following relationships from the INVIAS specifications, residue penetration, increase in the softening point, and residual asphalt viscosity aging index, were modified to penetration index (IP), softening index (IA), and viscosity index (IV), respectively, by dividing the value of the aged property by the nonaged RTFOT property, such that dimensionless values are obtained.

2.2. Structural Characterization through High Resolution ¹**H NMR.** ¹H NMR spectra were acquired with a Bruker Avance III NMR spectrometer, which operates at 400.16 MHz, and it is equipped with a 5 mm probe. The samples were diluted with deuterated chloroform, CDCl₃ (Merck, 99.8%), in an w/w ratio (sample:solvent) of 1:20, using tetramethylsilane (TMS) as the internal reference pattern. The sequence of pulses zg30 (Bruker) was employed to obtain the spectra, whose instrumental parameters are shown in Table 1.

Table 1. Set of Parameters Used in the Acquisition of the VR $^1\mathrm{H}$ NMR Spectra

parameter	value
number of points	32000
spectral width	15 ppm
time between pulses, D1 (s)	10 s
number of scans	32

Finally, the free induction decay (FID) of each sample was obtained. The FID of each sample was processed with the MestReNova program, to obtain the spectrum, as shown in Figure 1. Table 2 shows the spectral ranges, the frequencies, and the kind of protons corresponding to the 12 integration areas, applied to all the ECP and MPI samples. This procedure was conducted 10 times for each spectrum, so that a variation quotient smaller than 5% is guaranteed.

2.3. Relaxometric Properties through Low-Resolution NMR. The relaxometric data were taken in a Bruker Minispec mq NF 4093 spectrometer, with 0.17 T and 7.5 MHz, at the hydrogen frequency. The ECP and MPI samples were added directly to the sample holder tube. The spectrometer operates at a temperature of 40 °C with a deviation of ± 0.001 °C. The employed pulse sequence to obtain the T_2 relaxation plots was the Carr–Purcell–Meiboom–Gill (CPMG), which corresponds to the t2_cpmg_table_mq.app of the Minispec software. Table 3 shows the acquisition conditions for the low-resolution measurements.

The gain (RG) was adjusted by employing the "tune gain" routine of the device, and the acquisition time (AT) was adjusted to guarantee a full decay of the signal for each sample. To adjust the RD, the T_1 relaxation time was first measured, using the spectrometer routine t1_invrec_table_mq.app. In particular, the T_1 acquisition conditions were set as initial time 0.018 ms and final acquisition time 0.5 s, and 100 points were acquired. A relaxation time of T_1 = 30.3 ms was obtained for the VR. Finally, the magnetization time (or RD) employed was 0.15 s for the CPMG pulse sequence.

The T_2 relaxation curves obtained via the CPMG sequence were transformed into T_2 distribution plots by means of the inverse Laplace transform (ILT). For this, the Contin_ILT spectrometer routine was used, which employs the Tikhonov regularization method. The determination of the regularization α (alpha) parameter is automati-

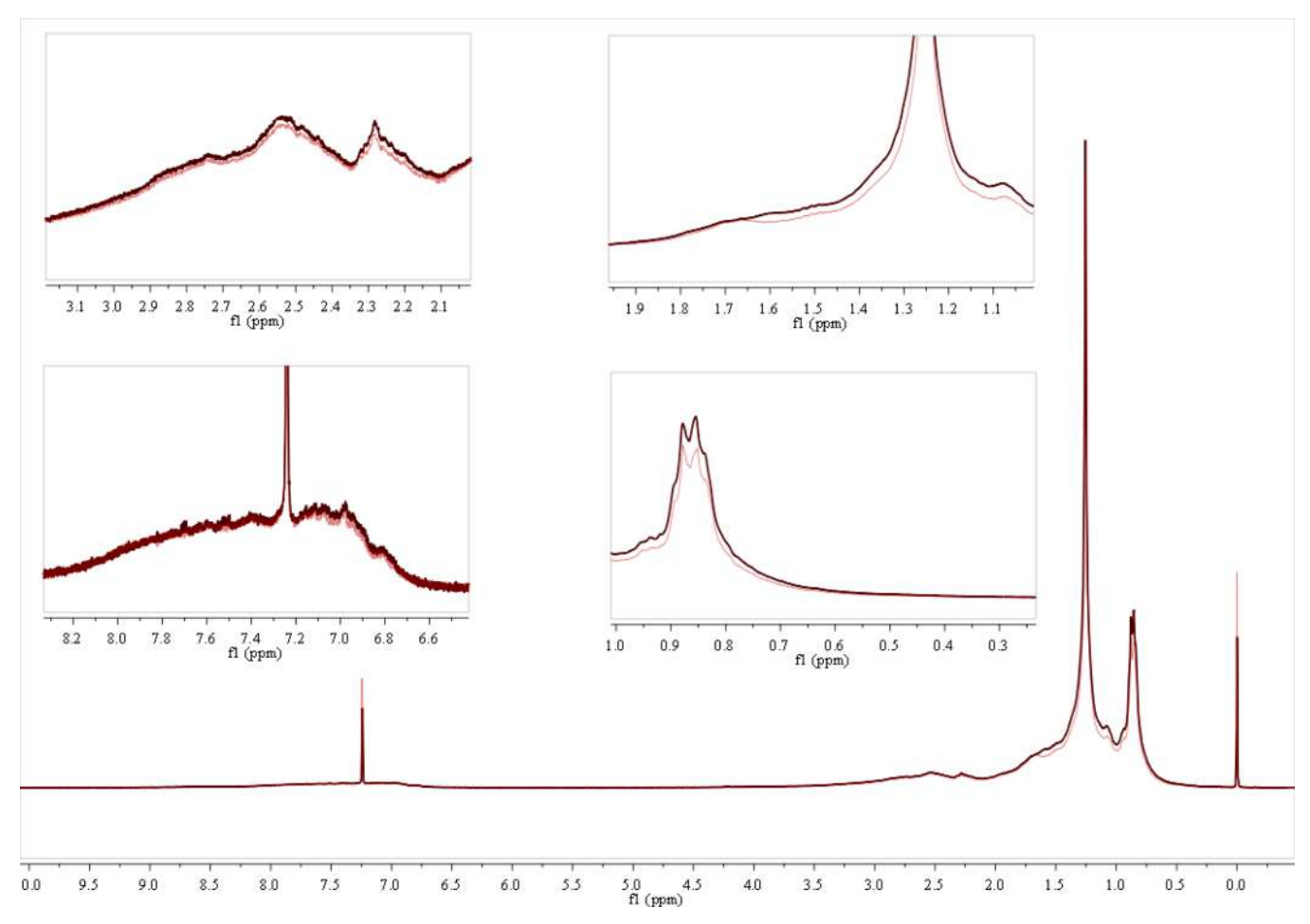


Figure 1. ¹H NMR spectra of the ECP1 (in black) and MPI1 (in red) samples.

Table 2. Spectral Ranges and Kind of Hydrogen Assigned to the ¹H NMR Spectra ²⁵

chemical shift (ppm)	nomenclature	hydrogen kind
0.5-1.0	H1	CH ₃ of paraffins (n- and iso-); paraffinic hydrogens γ for aromatic systems
1.0-1.7	H2	CH ₂ of paraffins (n- and iso-), CH of iso- paraffins, CH and CH ₂ of naphthenes, paraffinic hydrogens β for aromatic systems
1.7-1.9	Н3	CH and CH $_2$ of naphthenes; mainly β -CH and β -CH $_2$ for aromatic systems
1.9 - 2.1	H4	α -CH ₂ of olefins
2.1 - 2.4	H5	α -CH $_3$ for aromatic carbons
2.4 - 3.5	Н6	α -CH and α -CH $_2$ for aromatic carbons
3.5 - 4.5	H7	bridge CH ₂ or CH
4.5-6.0	H8	CH and CH ₂ of olefins
6.0 - 7.2	H9	CH of mono aromatic rings
7.2-8.3	H10	CH of diaromatic rings and some tri- and tetra-aromatic rings
8.3-8.9	H11	CH of some tri- and tetra-aromatic rings
8.9-9.3	H12	CH of some tetra-aromatic rings

cally defined by the software, and the outcome of the transformation is a plot of the f values versus T_2 that vary exponentially. Five hundred exponential terms, in the range of 0.01 to 1000 ms, were employed for all the samples.

An array of data was calculated by means of numerical integration, through continuous trapeziums at 100 intervals, for all the T_2 relaxation curves and distribution plots. This procedure was

Table 3. Acquisition Parameters Used by the CPMG T_2 Sequence

parameter	value
number of scan (NS)	512
gain (RG)	68 dB
R. delay (RD)	0.15 s
acquisition time (AT)	100 ms
echo time (ET)	0.05 s
number of echoes (NE)	1000
obtained data	1000

performed in order to define a short-range of data that included information about the intensity and time of the signal. The distribution plots along the 100 intervals were normalized by expressing the f values as dictated by eq 1:

$$f_{\text{Normalized}} = \frac{f_i}{\sum_{j}^{100} f_i} \tag{1}$$

The T_2 relaxation times of each peak were determined along with their corresponding relative area from the T_2 distribution plots, identifying them as t1, t2, t3 and A1, A2, and A3, respectively.

2.4. Multiple Correlation and Principal Components Analysis. The NMR data were analyzed via multiple correlation analysis (MCA) and principal components analysis (PCA). The physicochemical properties were set as the dependent variables (detailed in Section 2.1), and the independent variables were the $^{\rm 1}H$ NMR 12 integration areas (detailed in Section 2.2), as well as the times and areas of the T_2 distribution plots (t1, t2, t3, A1, A2, and A3,

Table 4. Descriptive Statistics of the Physicochemical Properties for the VR Samples^a

												INV inte	
property	standard	sample	average	variance	DS	CV, %	SE	min.	max.	standardized kurtosis	bias	min.	max.
P (0.1 mm)	ASTM D5	ECP	67.30	15.67	3.96	6	0.49	60	75	-0.83	0.20	60	70
,		MPI	66.94	2.38	1.54	0.02	0.19	62	70	1.51	-0.72		
A (°C)	ASTM D36	ECP	49.49	0.78	0.89	2	0.11	47.8	51.6	-0.62	-0.12	48	54
		MPI	49.79	0.15	0.38	0.01	0.05	48.4	50.8	3.72	-0.77		
Ip	NLT 181	ECP	-0.62	0.03	0.17	-27	0.02	-1.05	-0.28	-0.46	-0.02	-1.2	0.6
		MPI	-0.55	0.01	0.10	-0.19	0.01	-0.88	-0.25	2.71	-0.36		
V (cP)	AASHTO T316	ECP	2265	104445	323	14	40.4	1708	3024	-0.52	0.51		
		MPI	2288	29515	171.8	0.08	21.48	1962	2739	0.01	0.66		
R (%)	ASTM D2872	ECP	0.43	0.05	0.22	50	0.03	0.20	1.02	2.46	1.45		0.8
		MPI	0.40	0.02	0.16	0.39	0.02	0.21	0.80	2.49	1.64		
PR (0.1 mm)	ASTM D5	ECP	38.92	8.52	2.92	7	0.36	31	44	0.31	-0.61		
		MPI	38.38	1.83	1.35	0.04	0.17	33	41	5.20	-1.20		
AR (°C)	ASTM D36	ECP	56.69	2.54	1.59	3	0.20	53.8	63.0	6.39	1.40		
		MPI	56.95	0.96	0.98	0.02	0.12	54.4	58.8	-0.50	0.01		
VR (cP)	NLT 181	ECP	8139	12594100	3548	44	443.6	4953	25336	25.20	3.60		
		MPI	7718	1522910	1234	0.16	154.3	6082	10828	-0.88	0.77		
IP		ECP	0.58	0.00	0.04	7	0.00	0.47	0.69	4.23	-0.51		
		MPI	0.57	0.00	0.02	0.03	0.00	0.52	0.60	4.37	-1.47		
IA		ECP	1.15	0.00	0.03	2	0.00	1.07	1.26	9.64	1.28		
		MPI	1.14	0.00	0.02	0.02	0.00	1.12	1.18	-1.59	0.26		
IV		ECP	3.55	1.54	5	5	0.16	2.50	10.10	34.33	4.36		
		MPI	3.56	0.15	0.11	0.11	0.05	2.80	4.00	-1.77	0.66		

"DS – standard deviation, CV – variation quotient, A – softening, Ip – penetration index, Pe – specific weight, V – viscosity, R – RTFOT, PR – penetration RTFOT, AR – softening RTFOT, VR – viscosity RTFOT, IP – P/PR ratio, IA – A/AR ratio, IV – V/VR ratio.

detailed in Section 2.3). For the MCA, the Pearson (r) and Spearman (r_s) correlation coefficients were employed along with the P-value, to determine the 95% significance, and the relationship between pairs of variables was determined. The software used to conduct both MCA and PCA was STATGRAPHICS.

3. RESULTS AND ANALYSIS OF RESULTS

3.1. Characterization of the Physicochemical Properties of the Vacuum Residues. Table 4 shows the statistics of the physicochemical properties measured in this work. It can be observed that the standardized kurtosis showed significant deviations from the average for the R, AR, VR, IP, IA, and IV properties of the ECP samples and for the A, Ip, R, PR, and IP properties of the MPI samples. The standardized kurtosis converts the kurtosis (g_2) to a value that has approximately normal distribution (z_2), with a significance level of 95%; thus, a significant kurtosis is obtained if z_2 is out of the interval [-2, 2].

From Table 4, it may be observed that, after the VR are processed in the MPI facility, the average penetration value decreased 0.4 tenths of a millimeter, which means that a certain hardening occurred, implying an increase in the softening point (0.3 °C in average) and in the viscosity (22.3 cP in average). The same behavior was observed in the RTFOT values but this time due to the loss of volatiles during the VR aging.

Figure 2 shows the frequency histograms (polygons) of the physicochemical properties for the ECP and MPI samples. The choice of the class interval was made following the Scott's rule (based on normality) and Sturges. The two values shown in each histogram legend refer to the mode of the data: the first one is the average value of the property at the maximum

frequency, and the second one is the number of samples with the value of the maximum frequency.

It can be observed from Table 4 and Figure 2 that the MPI samples exhibit a smaller variability range for most of the properties than that of the ECP samples. Also, their maximum and minimum values are within the intervals demanded by INVIAS, and their bias keeps the same orientation (+ or –) for all of them but penetration; besides, the frequency of their mode is greater for all their properties. This indicates that the range of variability of the refinery VR properties did not meet the INVIAS specifications, to be employed as raw materials in the manufacture of pavements. In contrast, after the VR were treated in the MPI facility, their dispersion decreased, the number of samples within the quality intervals increased, and all of the MPI samples fulfilled the required quality for all the properties.

Regarding the INVIAS quality requirement, it is observed that after processing the VR in the MPI facility, all the properties adjust to the specification ($60 \le P \le 70$; $48 \le A \le 54$; $-1.2 \le \text{Ip} \le +0.6$; $R \le 0.8$; residue penetration in percentage of the original asphalt penetration (%) ≥ 50 ; increase in the softening point (°C) ≤ 9 ; aging index: viscosities ratio (60 °C) between the residual asphalt and the original asphalt (dimensionless) ≤ 4).

The RTFOT (R) property of the MPI samples showed greater values of mass loss, since additives or organic solvents with low molecular weight are used, in addition to the extra aging process. Properties of the residues, as per the RTFOT method, showed that RTFOT penetration exhibits a lower number of data at greater values, for the ECP samples, greater temperatures for RTFOT softening for MPI samples, and greater values in RTFOT viscosity for the ECP samples.

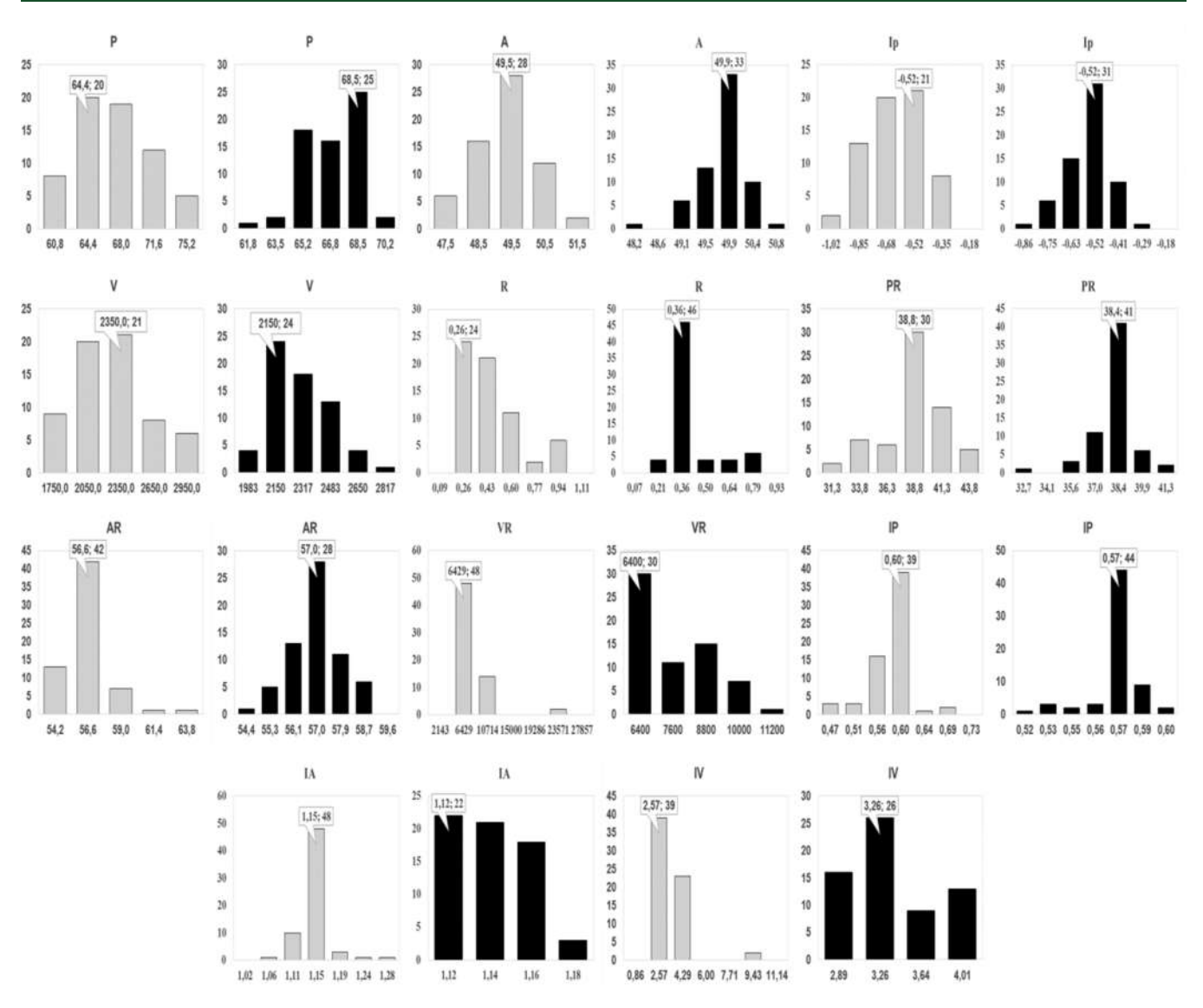


Figure 2. Frequency histograms for the physicochemical properties obtained from the VR of ECP (gray bars) and MPI (black bars).

Table 5. Correlations between the Properties for the VR Samples^a

	ECI	o^b	MI	PI ^b		I	ECP ^b	M	IPI ^b
correlation between	R	$r_{\rm s}$	r	$r_{\rm s}$	correlation between	r	$r_{\rm s}$	r	$r_{\rm s}$
P-A	-0.7				R-PR				-0.4
P-V	-0.7				R-IP		-0. 7		-0.6
P-PR	0.5				R-IA		0.4		
P-IA			0.3		R-IV		0.5		
P-IV			0.3		PR-IP				0.6
A-Ip	0.8			0.8	AR-VR		0.6	0.5	
A-V	0.7				AR-IA		0.6	0.9	
A-PR	-0.4				AR-IV		0.4	0.7	
Ip-V	0.3				VR-IA		0.3	0.5	
Ip-IV			0.3		VR-IV		0.8	0.9	
V-PR	-0.4				IP-IA		-0.3		
V-VR			0.7		IP-IV		-0.4		
V-IV			0.4		IA-IV		0.4	0.7	
R-VR		0.3							

 $[^]a$ r = Pearson coefficient; r_s - Spearman coefficient, P - penetration, A - softening, Ip - penetration index, P_e - specific weight, V - viscosity, R - RTFOT, PR - RTFOT penetration, AR - RTFOT softening, VR - RTFOT viscosity, IP - P/PR ratio, IA - A/AR ratio, IV - V/VR ratio. b Samples.

Table 6. Descriptive statistics for ¹H-NMR spectral ranges of the VR samples^a

proton kind	sample	average	variance	DS	CV, %	SE	mín.	max.	standardized kurtosis	bias
H1	ECP	21.50	0.21	0.45	2	0.06	20.69	22.48	-1.2	0.43
	MPI	21.44	0.301	0.55	3	0.07	20.22	22.55	-0.2	-0.04
H2	ECP	52.51	0.49	0.70	1	0.09	50.93	53.93	-1.0	-0.01
	MPI	52.46	0.44	0.66	1	0.09	51.00	53.71	-0.7	-0.44
H3	ECP	4.43	0.01	0.08	2	0.01	4.22	4.59	0.05	-0.64
	MPI	4.47	0.01	0.12	3	0.01	4.18	4.70	-0.8	-0.52
H4	ECP	2.38	0.01	0.07	3	0.01	2.26	2.54	-0.6	0.32
	MPI	2.38	0.01	0.08	3	0.01	2.22	2.56	-1.3	0.09
H5	ECP	3.33	0.01	0.09	3	0.01	3.16	3.54	-0.6	0.20
	MPI	3.32	0.01	0.10	3	0.01	3.11	3.52	-0.8	-0.29
H6	ECP	8.50	0.04	0.21	2	0.03	8.08	9.11	0.3	0.37
	MPI	8.52	0.07	0.26	3	0.03	7.96	9.28	1.5	0.54
H7	ECP	0.96	0.01	0.05	6	0.01	0.84	1.12	0.6	0.36
	MPI	0.94	0.01	0.07	7	0.01	0.82	1.09	-1.4	0.24
H8	ECP	0.11	0.01	0.01	12	0.01	0.07	0.14	1.2	0.05
	MPI	0.11	0.01	0.02	16	0.01	0.08	0.17	0.5	0.77
H9	ECP	2.18	0.01	0.07	3	0.01	2.06	2.39	1.4	0.90
	MPI	2.20	0.01	0.08	4	0.0097	2.04	2.44	1.1	0.33
H10	ECP	3.34	0.02	0.14	4	0.0176	3.06	3.77	1.6	0.53
	MPI	3.38	0.02	0.14	4	0.0173	3.15	4.08	15.9	2.31
H11	ECP	0.61	0.01	0.03	5	0.0036	0.54	0.69	1.9	0.13
	MPI	0.62	0.01	0.03	4	0.0034	0.57	0.75	15.0	1.97
H12	ECP	0.15	0.01	0.01	6	0.0011	0.13	0.17	0.03	-0.20
	MPI	0.15	0.01	0.01	5	0.0010	0.13	0.18	0.9	0.03
aDS – standar	d deviation	CV – vari	ation coefficie	ont II – 1	mimodo					

^aDS – standard deviation, CV – variation coefficient, U – unimode.

The MPI samples should exhibit greater viscosity values. The Ip showed lower average values with greater frequencies for the MPI samples. The IA slightly decreased for the MPI samples with lower frequencies, and the IV increased for the MPI samples. The penetration, softening, and viscosity properties show discrepancies with the logical trends that these materials should exhibit; however, this is explained since additives were added to the MPI samples to reduce their viscosity, thus causing an increase in penetration and softening.

3.2. Multiple Correlation Analysis. The correlation coefficients of Pearson (r - normal distributions) and Spearman $(r_s - \text{non-normal distributions})$ were employed to confirm the correlations between two properties. The correlations obtained between the properties are summarized in Table 5. Correlation values greater than 0.42 indicate high correlation, correlation values between 0.32–0.41 indicate moderate correlation, and correlation values less than 0.31 indicate low correlation.

It can be seen in Table 5 that, for the ECP samples, the penetration is inversely correlated with the softening (-0.7) and viscosity (-0.7) and directly correlated with the RTFOT penetration (0.5). For the MPI samples, the penetration is directly correlated with the softening (0.3) and the viscosity (0.3). The latter is caused by the aging process.

It is observed that for both ECP and MPI samples, the softening property is susceptible to temperature. The property Ip directly correlates with viscosity (0.3) for the ECP samples and with the viscosity index (0.3) for the MPI samples. This outcome is interesting since it shows correlation between Ip and IV. Hamzah and Shahadan²⁸ conducted a study of the physicochemical properties and, via Fourier-transform infrared spectroscopy (FTIR), of VR modified with asphalt of Recovered Asphaltic Pavement (RAP) and subjected them to diverse aging conditions. They found that the penetration

decreases and the softening point increases consistently in each oxidation level and also that the penetration index (Ip) and the viscosity aging index (IV) increase as the RAP modified binding agents age. Further, they found a significant correlation between the penetration index (Ip) and the viscosity aging index (IV) of 0.8, between the penetration index (Ip) and the area ratio of the spectral regions of the RAP modified binding agents of 0.7, and between the high viscosity aging index (IV) and the area ratio of the RAP modified binding agents of 0.5.

In the ECP samples, the viscosity property correlates with the RTFOT penetration (-0.4), and in the MPI samples, it correlates with both the RTFOT viscosity (0.7) and the viscosity index (0.4). It was observed for the MPI samples that the RTFOT viscosity and the viscosity index decreased, confirming that the expected logical trend was not followed probably due to the added additives that decreased viscosity.

Finally, the Ip does not correlate with the IV for the ECP samples but correlates loosely for the MPI samples (0.3), thus indicating the increase in viscosity. It is likely that the additive in the MPI samples is causing the loose coefficient and the behavior seen in the penetration and softening properties.

3.3. ¹H NMR Spectral Characteristics of Vacuum Residues. Note that the ¹H NMR spectra of the ECP and MPI samples, shown in Figure 1, present bands on the same chemical shifts (δ , ppm), even though the value of the integration areas varies among the samples. Table 6 shows the descriptive statistics of the integration areas relative to the 12 spectral ranges (H1, H2, H3, ..., H12) of all the samples, and Figure 3 depicts their histograms.

It can be observed in Table 6 and Figure 3 that the range of most of the properties for the MPI samples is smaller than those of the ECP samples and that the bias keeps the same orientation (+ or -) except for the ranges H1, H5, and H12. For H11 (CH of some tri- and tetra-aromatic rings), the mode

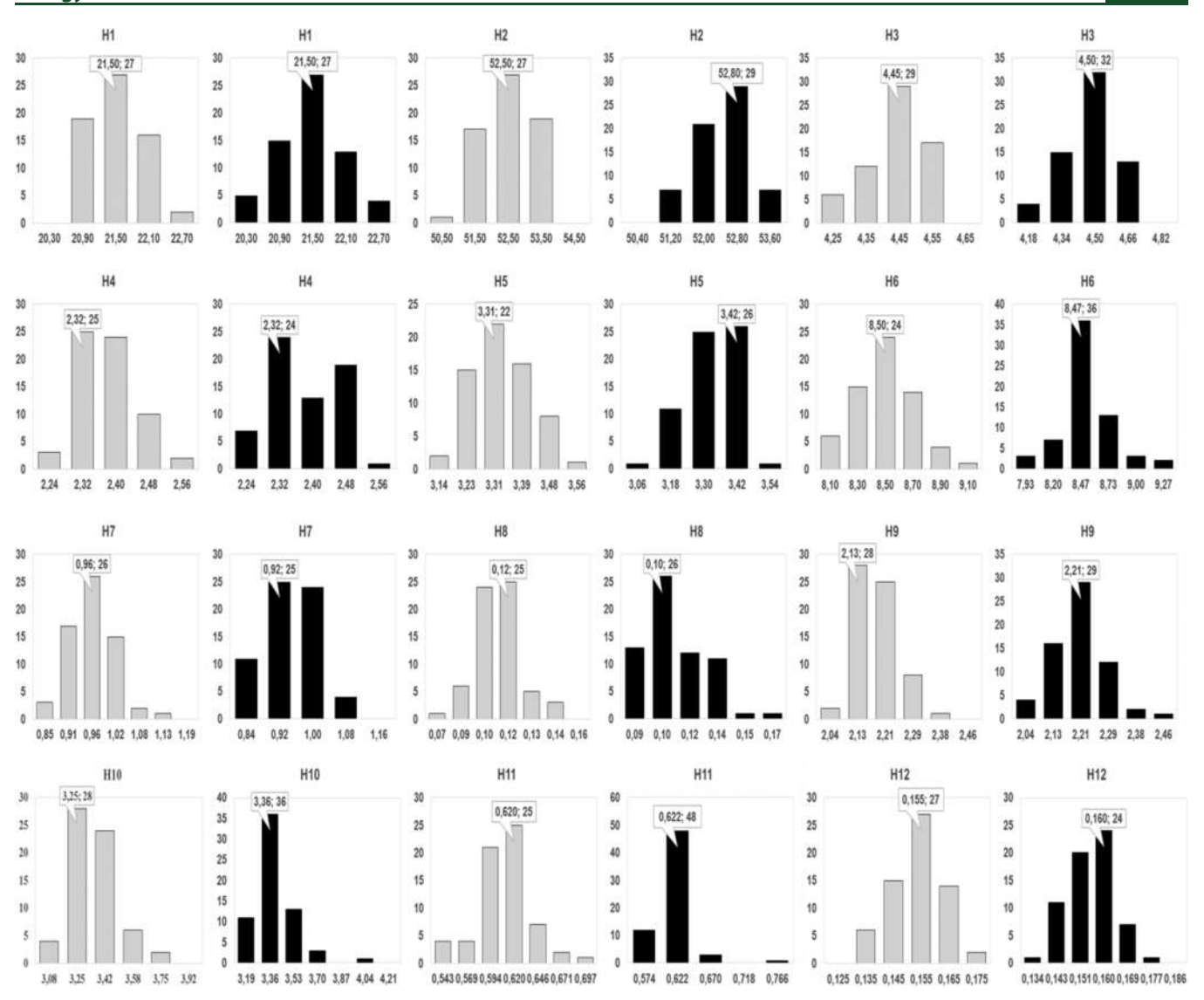


Figure 3. Histograms of the parameters from the structural composition of the VR from ECP (gray bars) and MPI (black bars), obtained from their ¹H NMR spectra.

remained the same, but its frequency was the one that increased the most. The latter probably indicates that the H11 range was the part of the molecules that was affected most by the aging process executed in the MPI facilities.

In Table 6 it can be also observed that the spectral ranges for the MPI samples exhibit normal distributions except for H10 and H11. The average number of protons of the MPI samples has larger values in the spectral ranges H3, H6, H9 to H12, which correspond to the aliphatic and olefinic protons and also to the compounds of mono-, di-, tri-, and tetra-aromatic rings. Instead, in the ECP samples prevail the ranges H1, H5, and H7, which correspond to compounds with aliphatic and aromatic protons and CH₂ or CH bridges.

Figure 3 shows that the MPI samples exhibit greater frequencies in the H2, H3, H5, H9, H10, H11, and H12 ranges, while the ECP samples exhibit greater frequencies in H6, H7, and H8 ranges. This probably explain the variations of the penetration and softening properties and the decrease in the viscosity mentioned in the previous section. Also, the number of protons increased in the more complex functional groups, which match with the aging.

Puello²⁹ studied two Colombian and one Venezuelan asphalt, subjected to accelerated aging assays in the laboratory. They confirmed the changing mechanism in the SARA composition: saturated (\sim 13%) \rightarrow naphthene aromatics (\sim 35%) \rightarrow polar aromatics (\sim 40%) \rightarrow asphaltenes (\sim 12%), and the aromaticity indices increased while the aliphatic index decreased, as the sample aged.

Due to the chemical complexity of the crude oils, it is not possible to allocate each one of the bands in the ¹H NMR spectrum with respect to the specific molecular structure types, but there exists a reasonable demarcation among methyl protons (0.5–1.10 ppm), methylene (1.10–1.65 ppm), methine (1.65–2.3 ppm), and the aromatic fractions (6.0–8.5 ppm). Therefore, the spectrum was divided into 12 chemical shift regions, proposed and used by different authors, including Meusinger. ³⁰ In his paper, the third crude studied (asphaltenes = 14.2%) has similar composition features to the VR studied in this paper. Meusinger concluded that differences in the chemical composition of crude oils may be easily detected in most of the spectral regions of the ¹H NMR, and such differences may be used to distinguish their chemical differences with high accuracy.

Smirnov and Vanyukova³¹ studied the distribution of the data and the degree of correlation of 14 compositional features of ¹H NMR and ¹³C NMR spectral data of Western Siberia crude oils. They showed that the parameters distribution highly differs from the normal distribution and that they vary substantially, being that the aromatic components are the most complex ones. They also showed the need to calculate the Spearman correlation coefficient instead of the Pearson pair, to determine the degree of interrelation of the parameters. Further, they demonstrated the strong interrelation of many composition parameters and suggested to study, in detail, the feasibility of their use in the comparative analysis of crude oils samples.

In this research study, it was observed that the MPI samples have normal distributions except for the H10 (CH of diaromatic rings and some tri- and tetra-aromatic rings) and H11 spectral ranges (CH of some tri- and tetra-aromatic rings), as well as their physicochemical properties, despite the variability in the composition during the year of sampling of the crude oils and their vacuum residues.

Correlations between the Properties and the Chemical Structure. Table 7 presents the common correlations between the multiple physicochemical properties and the ¹H NMR spectral ranges for all of the ECP and MPI samples.

Table 7. Correlations between Properties and Spectral Ranges of the VR Samples

1	ECP	a	MPI	a	1	MPI ^a	
correlation between	r	$r_{\rm s}$	r	$r_{\rm s}$	correlation between	r i	rs
P-H3	0.3				AR-H3	0.3	
A-H3	-0.3				AR-H4	0.5	
A-H10	0.3				AR-H5	0.4	
A-H11	0.3				AR-H6	0.4	
A-H12	0.3				AR-H7	0.4	
V-H3	-0.5				AR-H8	0.4	
V-H4	-0.3		-0.4		AR-H12	0.4	
V-H5	-0.3		-0.4		IA-H1	-0.4	
V-H6	-0.3		-0.4		IA-H4	0.5	
V-H7			-0.3		IA-H5	0.3	
PR-H2	0.3				IA-H6	0.4	
PR-H4	-0.3		-0.4		IA-H7	0.4	
PR-H5	-0.4		-0.3		IA-H8	0.5	
PR-H6	-0.3		-0.3		IA-H9	-0.3	
PR-H9	-0.3				IA-H12	0.4	
PR-H10	-0.4				IV-H1	-0.2	
PR-H11	-0.3				IV-H8	0.4	
AR-H1			-0.3		IV-H12	0.3	
^a Samples.							

Table 7 shows that the correlations between the physicochemical properties and the type of proton (¹H NMR) exhibit moderate values for most of the variable pairs. This indicates that the spectral ranges might be considered as good independent variables to predict properties of both the ECP and MPI samples.

3.4. Relaxometric Features of the Vacuum Residues. As an example, Figure 4 shows the T_2 relaxation and distribution plots for the ECP1 and MPI1 samples. Table 8 shows the relaxometry data statistics of the ECP and MPI samples, including the T_2 relaxation times (t1, t2, and t3) and

their corresponding normalized areas (A1, A2, and A3). In addition, Figure 5 shows the data statistics histograms.

Each band in Figure 4(b) corresponds to a macroaggregate or family of molecules with similar relaxation properties, where the shorter spin—spin relaxation time (T_2) (0.13 ms < t1 < 0.30 for the ECP samples and 0.11 ms < t1 < 0.30 ms for the MPI samples) corresponds to more rigid fractions, probably to the asphaltenes fraction and hydrocarbons of high molecular weight. It is observed in Table 8 and Figure 5 that, due to the aging effect, the minimum T_2 decreased from 0.13 ms (ECP) to 0.11 ms (MPI), the frequency did not change, the area A1 increased 3.3% on average, and although the mode did not change, its frequency increased in 5 units. All of this indicates that the asphaltenes increased in quantity as well as in their structural complexity due to the effect of aging.

The longest T_2 relaxation times (2.92 ms < t3 < 19.15 ms for the ECP samples and 3.94 ms < t3 < 14.17 ms for the MPI samples) should correspond to the fraction of molecules with low molecular weight and structurally less complex. It is observed in Table 8 and Figure 5 that there was a decrease in the maximum T_2 , due to the aging effect, from 19.15 to 14.17 ms and a decrease of 3.9% in their relative area A3, which might be explained by the loss of the lighter molecules (longer T_2) due to evaporation from heating.

Intermediate times (0.44 ms < t2 < 1.86 ms for the ECP samples and 0.56 ms < t2 < 2.33 ms for the MPI samples) should correspond to the intermediate relaxation compounds. It is observed in Table 8 and Figure 5 that changes did not occur, or were negligible, in the average of the t2 relaxation time and the percentage of the relative area of A2, due to aging effect.

The characterization of bituminous materials, for their application, is still conducted via standardized empirical tests, since the chemistry of the VR is very complex due to the vast amount of different chemical compounds they contain. In fact, there are still two opposing points of view: the "homogenous" and the "nonhomogenous" models.³² The former describes the VR as a dispersed polar fluid (DPF) and explains the asphalt microstructure as a continuous association of polar molecules (asphaltenes) dispersed in a fluid of nonpolar molecules or with relatively low polarity. The temporary monotone dependence of the VR viscoelasticity was taken as a key argument to support the DPF model. However, the nonhomogenous model has received much more scientific validation, and currently, the VR colloidal image is the most accepted model.

Gentile et al.²⁴ focused on understanding the physicochemical interactions between two commercially available regenerating substances and the VR. In order to reach this goal, they conducted rheological tests and employed NMR through the application of the Laplace inverse transform to the spin—echo decay (T_2) . As expected, the extracted VR are harder than the fresh VR, the penetration property is lower, whereas the viscosity and softening temperatures are higher in the extracted as phalt

Qin et al.³³ studied the aging effect of the asphalt structure in the field and in the laboratory. They concluded that the observed rheological hardening is attributed to compositional changes within the asphalts as they age. Aging of asphalt may significantly affect the amount of asphaltenes and aromatics without altering the content of saturates and resins. Aging converts the aromatic components into toluene-soluble asphaltenes. Besides, aging in the field drastically increases

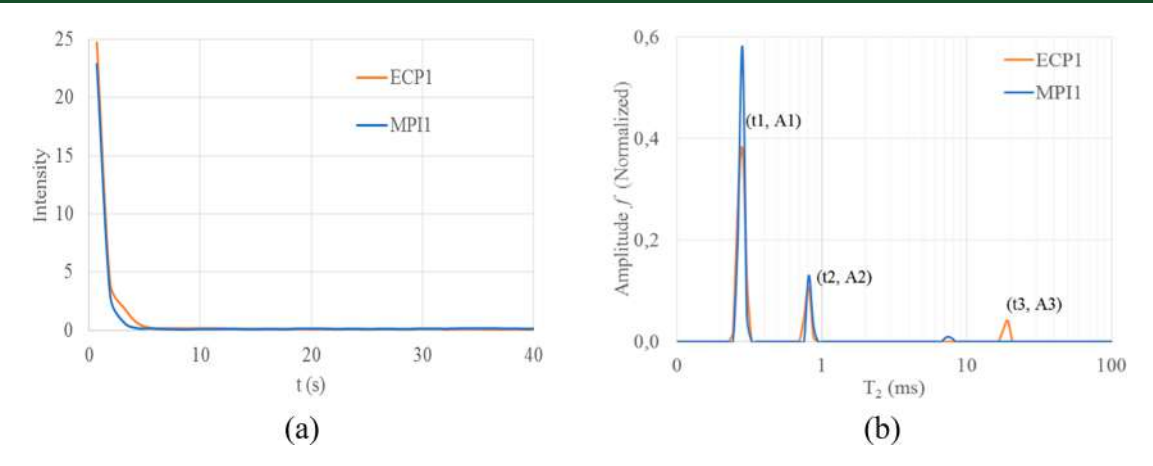


Figure 4. (a) T₂ relaxation and (b) T₂ distribution plots obtained by the CPMG sequence at 40 °C for the ECP1 and MPI1 samples.

Table 8. Descriptive Statistics for the Relaxometric Data of the VR Samples^a

property	sample	data	average	variance	DS	CV, %	SE	min.	max.	standardized kurtosis	bias
t1	ECP	63	0.26	0.002	0.05	17	0.006	0.13	0.3	3.3	-1.6
	MPI	64	0.27	0.002	0.05	17	0.006	0.11	0.3	7.6	-2.2
t2	ECP	38	0.83	0.09	0.3	36	0.05	0.44	1.86	6.7	2.2
	MPI	33	0.83	0.08	0.29	34	0.05	0.56	2.33	29.7	4.7
t3	ECP	24	6.4	10.5	3.24	50	0.66	2.92	19.15	10.4	2.9
	MPI	9	7.21	9.06	3.01	41	1.00	3.94	14.17	2.35	1.6
A1	ECP	63	83.6	380	19	23	2.45	28	100	2.36	-1.5
	MPI	64	86.9	376	19.4	22	2.43	26	100	4.87	-1.9
A2	ECP	38	25.4	403	20.1	79	3.25	2.0	72.0	0.26	1.1
	MPI	33	24.5	442.9	21.0	85	3.66	1.0	74.0	0.81	1.3
A3	ECP	25	6.64	363	19	287	3.81	1.0	98.0	25.3	4.9
	MPI	9	2.78	0.94	0.97	35	0.32	1.0	4.0	-0.0	-0.5

^aDS – standard deviation, CV – variation coefficient, U – unimode.

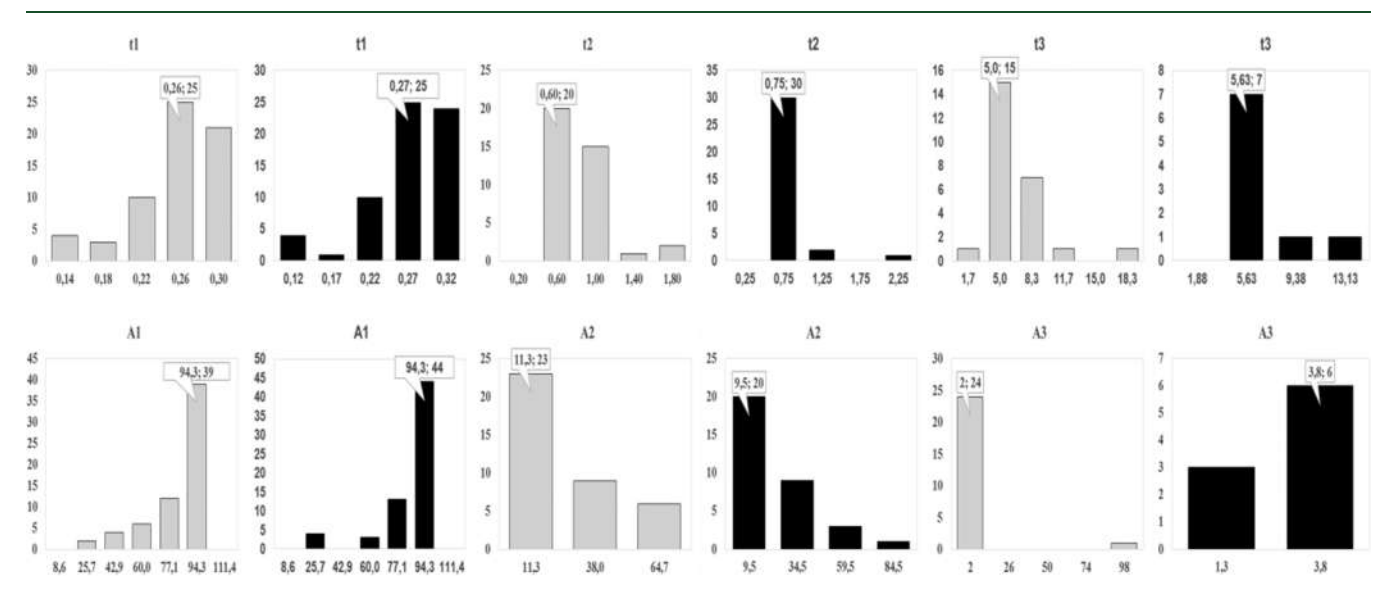


Figure 5. Histograms of the relaxometric parameters of the VR from ECP ECP (gray bars) and MPI (black bars), obtained from their T_2 distribution plots.

the total pericondensed aromaticity, as well as the carbonyl and sulfoxide functional groups.

Values obtained from the rheological method and the penetration/softening procedures are not equal. This is expected since the rheological analysis is conducted in the linear region of the material response, i.e., it is a non-perturbative observation, and it shows the intrinsic behavior of

the material. However, the penetration and softening properties are nonlinear/perturbed measurements. Rheological results confirm that the increase in the transition temperatures (fresh asphalt \rightarrow extracted, extracted + treated with additive) is the result of a greater fraction of asphaltenes, due to the oxidation processes of the soft-resinous materials. This asphaltenes enrichment might cause greater rigidity and

connectivity, when compared with the less dense network of the fresh VR, where the asphaltenes domains are poorly connected between each other. This finding weakens the DPF description of the VR structure. In fact, if the polar fluid model for our system were valid, the result of the T_2 relaxation time distribution would have been a single wide band referred to as a continuous T_2 time distribution.

Therefore, within the framework of the VR colloidal model, the shorter T_2 relaxation times should correspond to the asphaltenes fraction, whereas the longer relaxation times should correspond to the malthenes fraction. Intermediate T_2 times should represent resins, which are expected to have an intermediate mobility between asphaltenes and malthenes.

Morriss et al.³⁴ determined that a short echo time (TE) (320 μ s) will yield a greater sensitivity to any component with a very rapid decay. Studies have shown that T_2 time distributions, estimated at short TE, make the effect of molecular diffusion negligible. However, for high viscosity crude oils (>50,000 cP), it is believed that the deviation of the correlation between the viscosity and the T_2 distribution data is due to the experimental bias, associated with the very short spectrometer measurements. Since this bias was present in the relaxation data obtained for the VR used in this paper, the Spearman correlation coefficients were employed to confirm the correlations.

Table 9 shows the correlations between the physicochemical properties and the relaxation data. The penetration, softening,

Table 9. Correlations between the Properties and the NMR Data of the VR Samples^a

	EC	∑P ^b		ECP ^b		
correlation between	r	$r_{\rm s}$	correlation between	r	$r_{\rm s}$	
P-A2	0.4		1P-t1		0.3	
A-A2	-0.5		IA-t1		-0.3	
Ip-A2	-0.3		IA-t2		-0.4	
V-A2	-0.4		IV-t1		-0.3	
R-t1		-0.4	IV-t2		-0.4	
R-t2		-0.4				

^ar − Pearson coefficient; r_s − Spearman coefficient. ^bSamples.

Ip, and viscosity properties of the ECP samples have correlation with A2, that is, with the number of molecules with intermediate relaxation. For the ECP samples, the RTFOT, IP, IA, and IV properties are correlated with the t1 relaxation time, and the RTFOT, IA, and IV properties are correlated with t2. In general, low correlation is observed between the properties and the NMR data for the ECP samples and null correlation for the MPI samples.

Principal Components Analysis. Figure 6 shows the score graphs of the first two principal components (PC1, PC2) for the ECP and MPI samples, while Figure 7 shows the weights obtained from the kind of protons. The first component (PC1) explains 46% of the spectral variance for the ¹H NMR of the ECP samples and 50% of the MPI samples, whereas PC2 accounts for 23% and 22%, respectively. It is observed that they do not differ substantially.

PC1 showed greater variability for the ECP samples in the spectral ranges H2, H3, H6, H10, and H11, ranges associated with the ramified aliphatic compounds and to the aromatics of low and medium molecular weight. For the MPI samples, the greater values are exhibited by H1, H7, H8, and H12, ranges associated with the linear and cyclical aliphatic compounds,

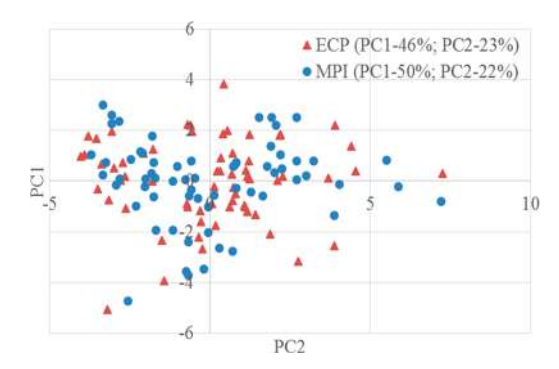


Figure 6. Score graphs of the principal components of the ¹H NMR for the ECP and MPI samples.

olefins, and high molecular weight polyaromatics. The second component (PC2) showed greater values in the H1, H8, H9, and H12 ranges for the ECP samples and in the H2 and H3 ranges for the MPI samples.

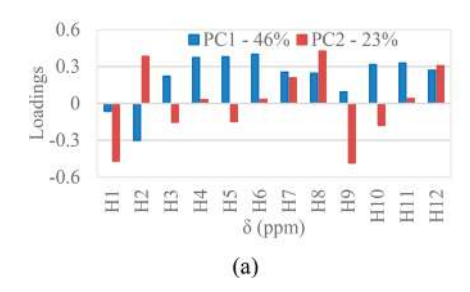
In general, it is observed that the ECP samples present greater functional groups variability in the spectral ranges H1–H7, which is very likely associated with the rich compounds in aliphatic protons and low molecular weight aromatics, while the MPI samples presented it on the functional groups within the H6–H12 ranges; however, they have variations in the ranges between H2 and H5, thus indicating that they have been further processed with additives, by heating in the facility.

4. CONCLUSIONS

Significant correlations (>0.6) were established between the physicochemical properties of the studied VR. In particular for the ECP samples, correlations were noted between penetration-softening (-0.7), penetration-viscosity (-0.7), softening-penetration index (IP) (-0.8), softening-viscosity (0.7), RTFOT-penetration index (IP) (-0.7), RTFOT softening-RTFOT viscosity (0.6), RTFOT softening-softening index (IA) (0.6), and RTFOT viscosity-viscosity index (IV) (0.8). Also, for the MPI samples, correlations were noted between softening-penetration index (Ip) (0.8), viscosity-RTFOT viscosity (0.7), RTFOT penetration-penetration index (IP) (0.6), RTFOT softening-softening index (IA) (0.9), RTFOT softening-viscosity index (IV) (0.7), RTFOT viscosityviscosity index (IV) (0.9), and softening index (IA)-viscosity index (IV) (0.7). Possibly, the MPI samples were treated with additives to decrease their viscosity in the facility processing; however, aging cannot be avoided.

Structural differences were determined among the spectral ranges obtained via ¹H NMR for such complex samples as the VR, which were confirmed by means of statistical correlation between the two materials studied. In general, the MPI samples presented greater concentrations of compounds with functional groups of resins and high molecular weight aromatics, whereas the ECP samples presented greater concentrations with aliphatic and monoaromatic functional groups. This was confirmed with the relaxometric data obtained by low-resolution NMR. The MPI samples presented a greater number of unimode distributions compared against the ECP samples.

Regarding the quality control of the properties for asphalts with penetration grade 60/70, it was observed that the MPI asphalts meet the specifications, while the ECP samples only satisfy the penetration index (Ip).



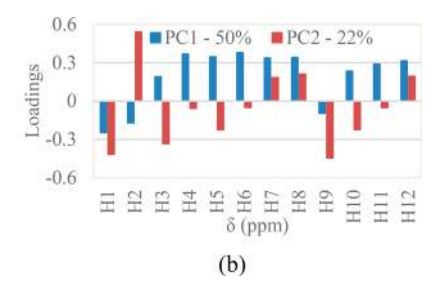


Figure 7. PCA for ¹H NMR spectral ranges. PC1 and PC2 for the (a) ECP and (b) MPI samples.

AUTHOR INFORMATION

Corresponding Author

*E-mail: dmolina@uis.edu.co.

ORCID ®

Daniel Molina V.: 0000-0002-7897-2526

Notes

The authors declare no competing financial interest.

ACKNOWLEDGMENTS

The authors acknowledge the research project "Advanced imaging techniques in porous media for nonintrusive characterization of rocks and increase in the recovery factor of heavy crude fields and conventional crude oils mature fields" with contract number RC. No. 0513 of 2013 between COLCIENCIAS and UIS with support of ECOPETROL S.A. The authors also thank Eng. Ricardo Carreño from the MPI Company, for providing the samples, and the Nuclear Magnetic Resonance Laboratory from the Universidad Industrial de Santander.

■ REFERENCES

- (1) Simanzhenkov, V. Processing of heavy crude oils and crude oil residues; Marcel Dekker, Inc.: 2003.
- (2) Vuković, J. P.; Novak, P.; Plavec, J. Croat. Chem. Acta 2015, 88 (1), 89–95.
- (3) Altgelt, K.; Boduszynski, M. Composition and analysis of heavy petroleum fractions; New York, 1994; 489p.
- (4) Boduszynski, M. M.; Altgelt, K. H. Energy Fuels 1992, 6, 72-76.
- (5) Podgorski, D. C.; Yuri, E.; Corilo, Y. E.; Nyadong, L.; Lobodin, V. V.; Bythell, B. J.; Robbins, W. K.; McKenna, A. M.; Marshall, A. G.; Rodgers, R. P. *Energy Fuels* **2013**, *27*, 1268–1276.
- (6) Boduszynski, M. M.; Mckay, J. F.; Lathan, D. R. Asphalt Paving Technol. 1980, 49, 123-143.
- (7) Silva, S. L.; Silva, A. M. S.; Ribeiro, J. C.; Martins, F. G.; Da Silva, F. A.; Silva, G. M. *Anal. Chim. Acta* **2011**, 707, 18–37.
- (8) El Akrami, H. A.; Yardim, M. F.; Ekinci, E. Fuel **2000**, 79, 497–504.
- (9) Friedel, R. A. J. Chem. Phys. 1959, 31 (1), 280-281.
- (10) Ramsey, J. W.; Mcdonald, F. R.; Petersen, J. C. Ind. Eng. Chem. Prod. Res. Dev. 1967, 6 (4), 231–236.
- (11) Herrington, P. R.; Patrick, J. E.; Ball, G. F. A. Ind. Eng. Chem. Res. 1994, 33, 2801–2809.
- (12) Siddiqui, M. N.; Ali, M. F. Fuel 1999, 78, 1407-1416.
- (13) Michon, L. C.; Netzel, D. A.; Turner, T. F.; Martin, D.; Pascal, J. Energy Fuels 1999, 13, 602-610.
- (14) Jennings, P. W.; Desando, M. A.; Raub, M. F.; Moats, R.; Mendez, T. M.; Stewart, F. F.; Hoberg, J. O.; Pribanic, J.A. S.; Smith, J. A. Fuel Sci. Technol. Int. 1992, 10 (4–6), 887–907.
- (15) Huang, S. C.; Miknis, F. P.; Schuster, W.; Salmans, S.; Farrar, M.; Boysen, R. *J. Mater. Civ. Eng.* **2011**, 23 (5), 628–637.
- (16) Zhang, F.; Hu, C. Construction and Building Materials 2015, 76, 330–342.

- (17) Wang, Y.; Yuan, Q.; Deng, D.; Ye, T.; Fang, L. Construction and Building Materials 2017, 137, 450-458.
- (18) Kashaev, R. S.; Khairullina, I. R. Pet. Chem. 2009, 49 (6), 507-511.
- (19) Menapace, I.; Masad, E.; Nogueira, M.; Galvosas, P.; Hunter, M. W.; Sirin, O. Study on the use of low field nuclear magnetic resonance for detecting asphalt aging. *Bearing Capacity of Roads, Railways and Airfields*; Loizos, A., et al., Eds.; Taylor & Francis Group: London, 2017; pp 1589—1596, ISBN 978-1-138-29595-7.
- (20) Menapace, I.; Masad, E.; Papavassiliou, G.; Kassem, E. Bituminous Mixtures & Pavements, VI; Nikolaides, A., Ed.; Taylor & Francis Group: London, 2015; pp 395–400, ISBN 978-1-138-29595-7, DOI: 10.1201/b18538.
- (21) Menapace, I.; Garcia, L.; Kaseer, F.; Masad, E.; Martin, A. E. Construction and Building Materials 2018, 170, 725-736.
- (22) Oliviero, C.; Spadarofa, A.; Teltayev, B.; Izmailova, G.; Amervayev, Y.; Bortolotti, V. *Colloids Surf., A* **2015**, 480 (5), 390–397.
- (23) Menapace, I.; Nogueira, M.; Galvosas, P.; Hunter, M.; Sirin, O.; Masad, E. *Mater. Charact.* **2017**, *128*, 165–175.
- (24) Gentile, L.; Filippelli, L.; Oliviero, C.; Baldino, N.; Ranieri, G. Mol. Cryst. Liq. Cryst. 2012, 558, 54–63.
- (25) Molina V, D.; Navarro Uribe, U.; Murgich, J. Fuel 2010, 89, 185-192.
- (26) Sturges, H. A. J. Am. Stat. Assoc. 1926, 21 (153), 65-66.
- (27) Pojić, M. M.; Spasojević, N. B.; Atlas, M. D. Food Bioprocess Technol. **2014**, 7, 1298–1309.
- (28) Hamzah, M. O.; Shahadan, Z. Aust. J. Basic Appl. Sci. 2011, 5 (5), 1323–1331.
- (29) Puello, J. Tesis de Doctorado en Ingenieria Quimica, Bucaramanga, Universidad Industrial de Santander, Facultad de Ingenierias Fisico Químicas, 2012.
- (30) Meusinger, R. Fuel 1996, 75 (10), 1235-1243.
- (31) Smirnov, M. B.; Vanyukova, N. A. Pet. Chem. 2014, 54 (1), 16–27.
- (32) Lesueur, D. Adv. Colloid Interface Sci. 2009, 145, 42-82.
- (33) Qin, Q.; Schabron, J. F.; Boysen, R. B.; Farrar, M. J. Fuel 2014, 121, 86-94.
- (34) Morriss, C.; Rossini, D.; Straley, C.; Tutunjian, P.; Vinegar, H. Log Analyst 1997, 38 (2), 44–59.